Three-Phase Compositional Simulation Modeling Coupled with Reactive Transport: Application to Farnsworth Field CO2-EOR and Storage Project

Eusebius Junior Kutsienyo[1], William Ampomah[2], Robert Balch[3], Martha Cather[1], and Andrew Luhmann[4]

[1]New Mexico Institute of Mining and Technology
[2]Petroleum Recovery Research Center, New Mexico Tech
[3]New Mexico Institute of Mining and Technology
[4]University of Minnesota

November 21, 2022

Abstract

This poster presents field-scale numerical compositional simulations of CO2 storage mechanisms in the Morrow B sandstone of the Farnsworth Unit (FWU) located in Ochiltree County, Texas. The study examines structural-stratigraphic, residual, solubility and mineral trapping mechanisms. The reactive transport modeling incorporated evaluates the field's potential for long-term CO2 sequestration and predicts the CO2 injection effects on the pore fluid composition, mineralogy, porosity and permeability. The dynamic CO2 sequestration simulation model was built from an upscaled geocellar model for the Morrow B. This model incorporated geological, geophysical, and engineering data including well logs, core, 3D surface seismic and fluid analysis. We calibrated the model with historical CO2-WAG miscible flood data and used it to evaluate the feasibility and mechanisms for CO2 sequestration. We used the maximum residual phase saturations to estimate the effect of gas trapped due to hysteresis. In addition, gas solubility in the aqueous phase was modelled as function of pressure, temperature and salinity. Lastly, the coupled geochemical reactions, i.e., the characteristic intra-aqueous and mineral dissolution/precipitation reactions were assimilated numerically as chemical equilibrium and rate-dependent reactions respectively. Additional scenarios that involve shut-in of wells were performed and the reservoir monitored for over 1000 years to understand possible mineralization. Changes in permeability as a function of changes in porosity caused by mineral precipitation/dissolution were calibrated to the laboratory chemo-mechanical responses. The study validates the effects of Morrow B petrophysical properties on CO2 storage potential within the FWU. Study results shows: EOR at the tertiary stage of field operations, total amount of CO2 stored in aqueous-gaseous-mineral phases, evolution and dissolution/precipitation of the principal accessory minerals and the time scale over which mineral sequestration took place in the FWU. This study relates the important physics and mechanisms for CO2 storage in the FWU and illustrates the use of the coupled reactive flow. The study serves as a is benchmark for future field-scale reactive transport CO2-EOR projects in similar fields throughout the world.

ABSTRACT ID: 380420   PAPER #: MR53A - 0104

Three-Phase Compositional Simulation Modeling Coupled with Reactive Transport

Application to Farnsworth Field CO_2-EOR and Storage Project

Eusebius Kutsienyo Jr. New Mexico Institute of Mining & Technology (NMT)
William Ampomah Petroleum Recovery Research Center (PRRC)
R.S. Balch, Martha Cather, PRRC
Andrew Luhmann , Wheaton College & NMT

ABSTRACT

This study presents results of field-scale numerical simulations of CO_2 storage in the Morrow B sandstone of the Farnsworth Unit (FWU) located in Ochiltree County, Texas. The study examines structural-stratigraphic, residual, solubility and mineral trapping mechanisms. The modeling, which incorporates geochemistry, evaluates the field's potential for long-term CO_2 sequestration and predicts the CO_2 injection effects on the pore fluid composition, mineralogy, porosity and permeability.

An upscaled geocellular model for the Morrow B was constructed from geological, geophysical, and engineering data including well logs, core, 3D surface seismic and fluid analysis. We calibrated the model with historical CO_2-WAG miscible flood data and used it to evaluate the feasibility and mechanisms for CO_2 sequestration.

The study validates the effects of Morrow B petrophysical properties on CO_2 storage potential within the FWU. Study results shows: Enhanced Oil Recovery at the tertiary stage of field operations, total amount of CO_2 stored in aqueous-gaseous-mineral phases, evolution with dissolution/precipitation of the principal accessory minerals and the time scale over which mineral sequestration took place in the FWU.

BACKGROUND [1,2,3]

FWU Reservoir Description

- Field discovered in October 1955
- Morrow sandstone deposited in an incised fluvial valley
- Diagenetic processes altered primary porosity and permeability
- Average porosity and permeability calculated as 14.53%, 48.2 mD respectively
- Overlying Morrow shale and Akotan Series shales/limestones provide excellent seal
- Productive area extends to ~ 8300 acres
- Pay zone maximum thickness is 54 ft, average is 22 ft
- Reservoir is water-wet system with no record of either oil-water or gas-oil contact

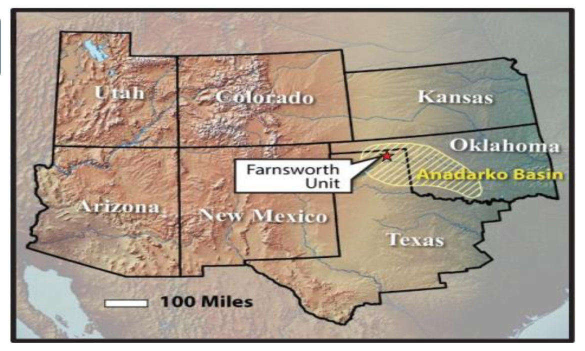

Figure 1: Location of FWU and 7 member states of that form SWP [2].

FWU Production History

- OOIP ~ 120 MMSTB, OGIP ~ 41.48 BCFG
- Initial reservoir pressure was 2203 psig at datum depth of 4900 ft
- Initial reservoir temperature recorded at 168 °F at irreducible water saturation of 31.4%
- Bubble point pressure at field discovery was 2059 psig
- Primary recovery by solution gas ~ started 1955
- Secondary recovery by waterflood ~ started January 1964
- Tertiary recovery by CO_2 flood ~ started December 2010

CO_2-EOR Compositional Modeling

- PVT Fluid tuned to EOS
- 174 x 161 x 15 grid cells (Fig 3)
- 100 ft x 100 ft block size
- Total number of active cells ~ 112,056
- 31 producers
- 20 injectors (16 WAG, 4-H_2O)
- 2-phase relative permeabilities (Figs 4 & 5)
- Segregated model used to calculated the 3-phase K_{ro}

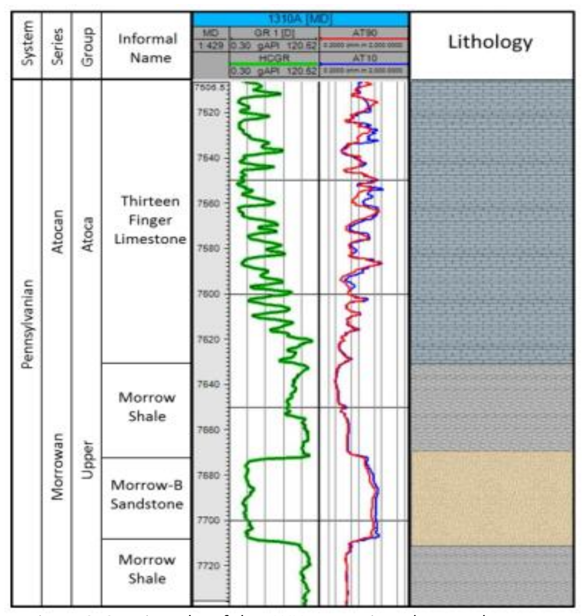

Figure 2: Stratigraphy of the FWU reservoir and cap rock

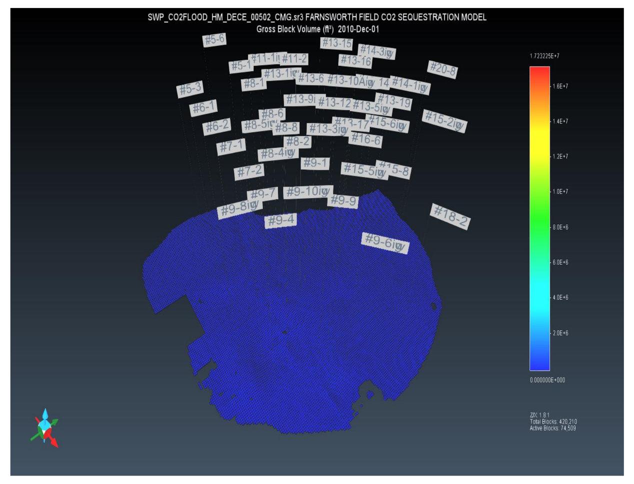
Figure 3: Compositional FWU reservoir model with well locations

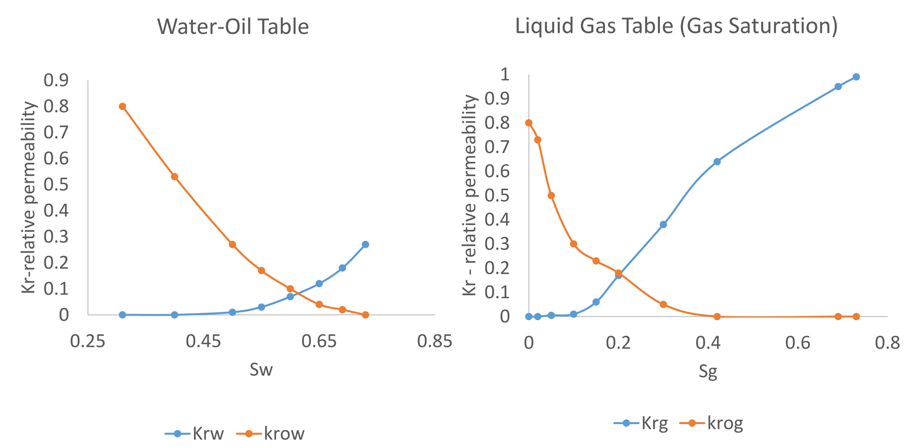

Figures 4 & 5 : Two Phase Relative Permeability curves for water-Oil and gas-liquid flow

METHOD

1. ASSISTED HISTORY MATCHING

Uncertainty Variables Considered in Sensitivity Studies

- ❑ Critical Saturations
- ❑ Permeability (I,J,K)
- ❑ Relative Permeability Curves
- ❑ Corey Exponents

Controlling Variables to Objective Function

- ❑ Corey Exponents
- ❑ Permeability(I,J)
- ❑ Critical saturation(e.g. Swcrit)
- ❑ Kr at Connate water / irreducible oil

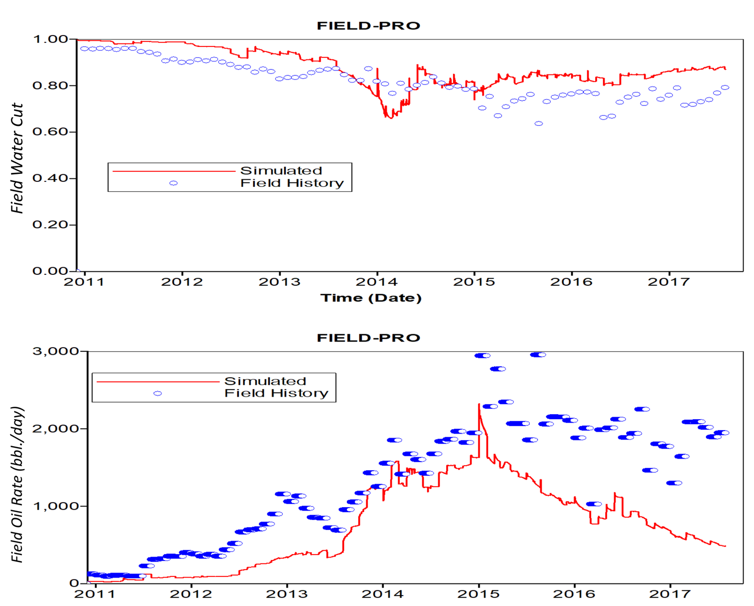

Figure 6. Base model simulating reservoir performance. Upper left: water cut during the base run. Lower left: field oil rate during the history period of seven years.

History Matching was performed for the base run results of CO_2 flood performance after using proxy models. Two optimization algorithms were applied using the same objective functions. Period of history is seven years

- **Design Exploration & Controlled Evolution (DECE) ~ 12% Overall Error**
- **Particle Swarm Optimization (PSO) ~ 10% Error**

History Match Results (DECE)

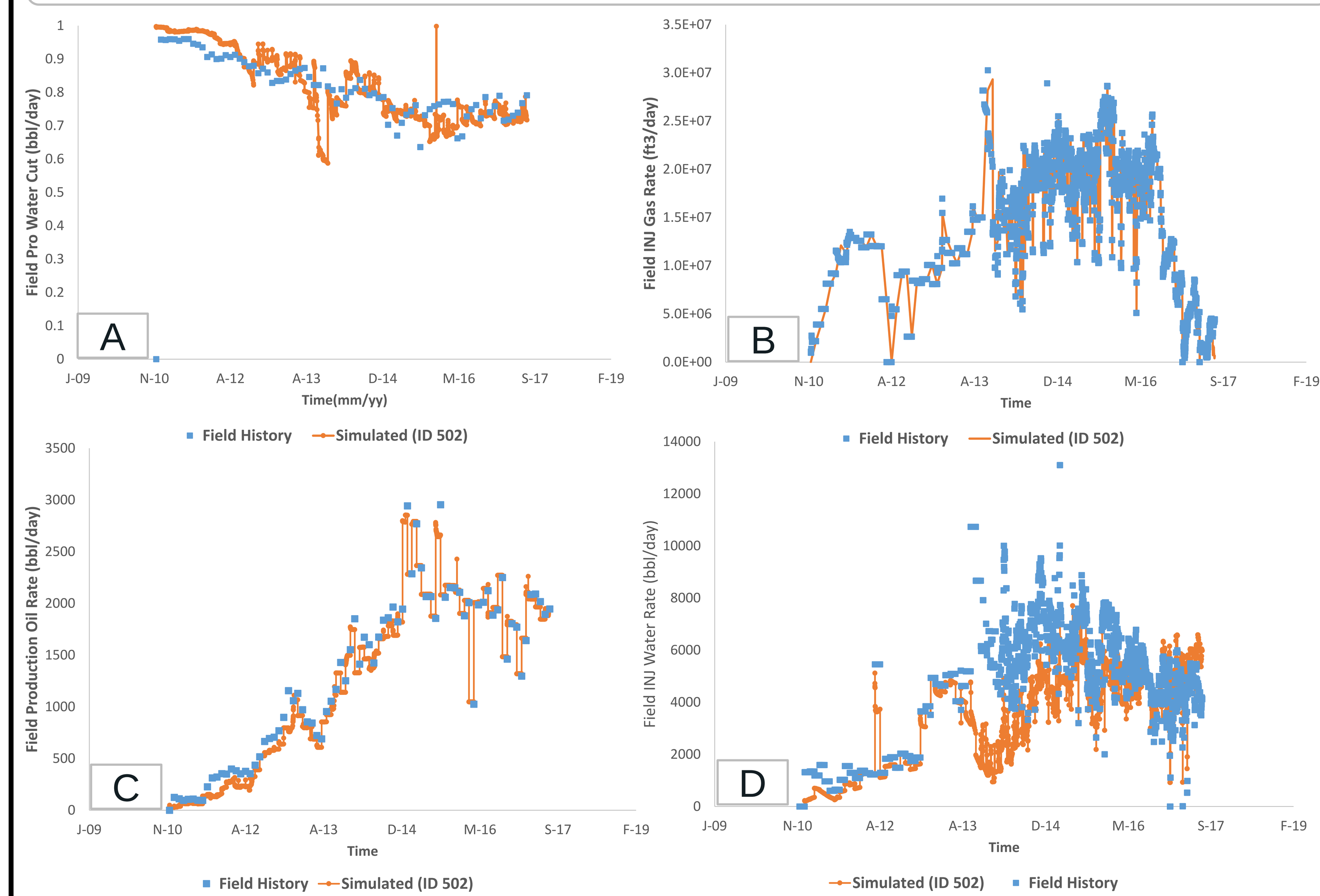

*Figure 7. History Match Reservoir Model showing actual and simulated performance of the reservoir field history for a seven-year period. **A:** Water cut, **B**: Gas injection rate, **C**: Field oil rate history match, **D**: Water injection rate.*

2. RESIDUAL GAS TRAPPING MODELING

2.1 Gas Phase Relative Permeability Hysteresis Modelling

- ❑ Lands hysteresis model (Lands Correlation [1])
- ❑ Carlson hysteresis model (CARLSON AND LANDS [1,2,3])
- ❑ Three-phase (3P) WAG model (Larsen and Kauge [6], Gas phase [1,2,3,4])
- ❑ $S_{gr} = S_{gcrit} + \frac{(S_{gm}-S_{gcrit})}{(1+C\,(S_{gm}-S_{gcrit}))} \ldots..(1)$ $K_{rg}(S_g) = K_{rg}^{drain}(S_{gf}) \ldots..(2)$ $S_{gf} = S_{gcrit} + \frac{1}{2}\left\{(S_g - S_{gr}) + \sqrt{(S_g - S_{gr})^2 + \frac{4}{C}(S_g - S_{gr})}\right\} \ldots\ldots(3)$
- ❑ $K_{rg}^{drain} = \left[K_{rg}^{input} - K_{rg}^{input}(S_g^{start})\right]\left[\frac{S_{wcon}}{S_w^{start}}\right]^{\alpha} + \left[K_{rg}^{imb}(S_g^{start})\right] \ldots\ldots..(4)$

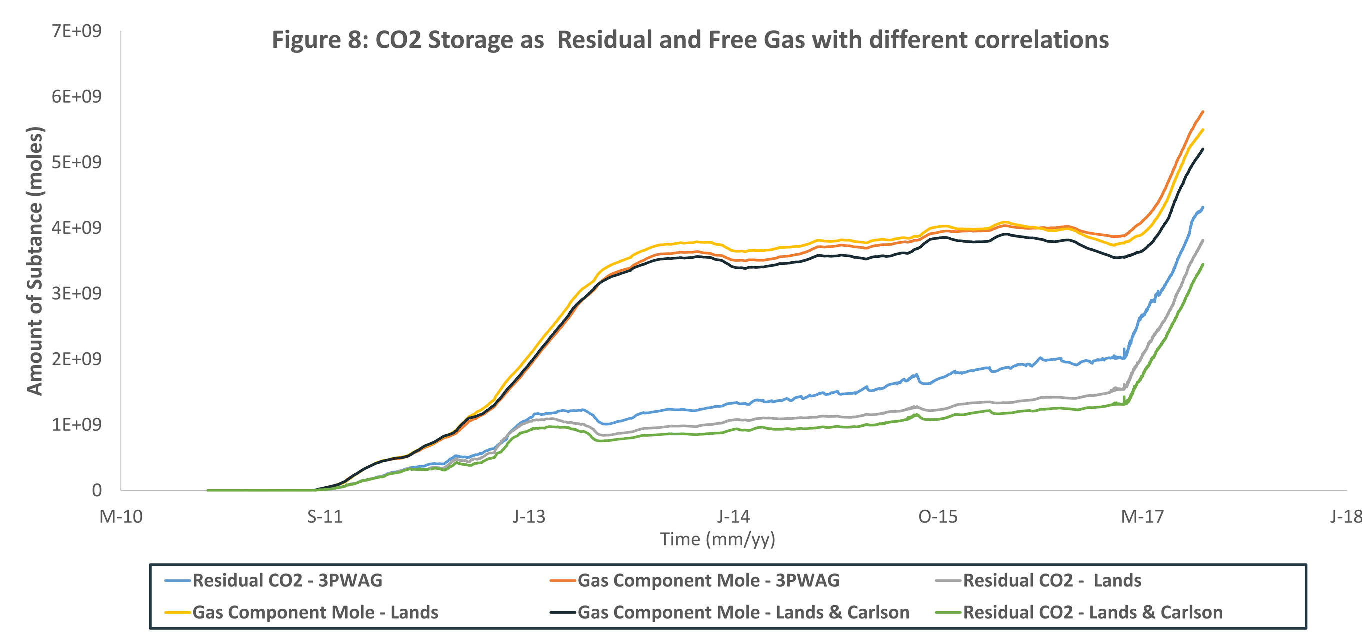

2.2 CO_2 storage modelling

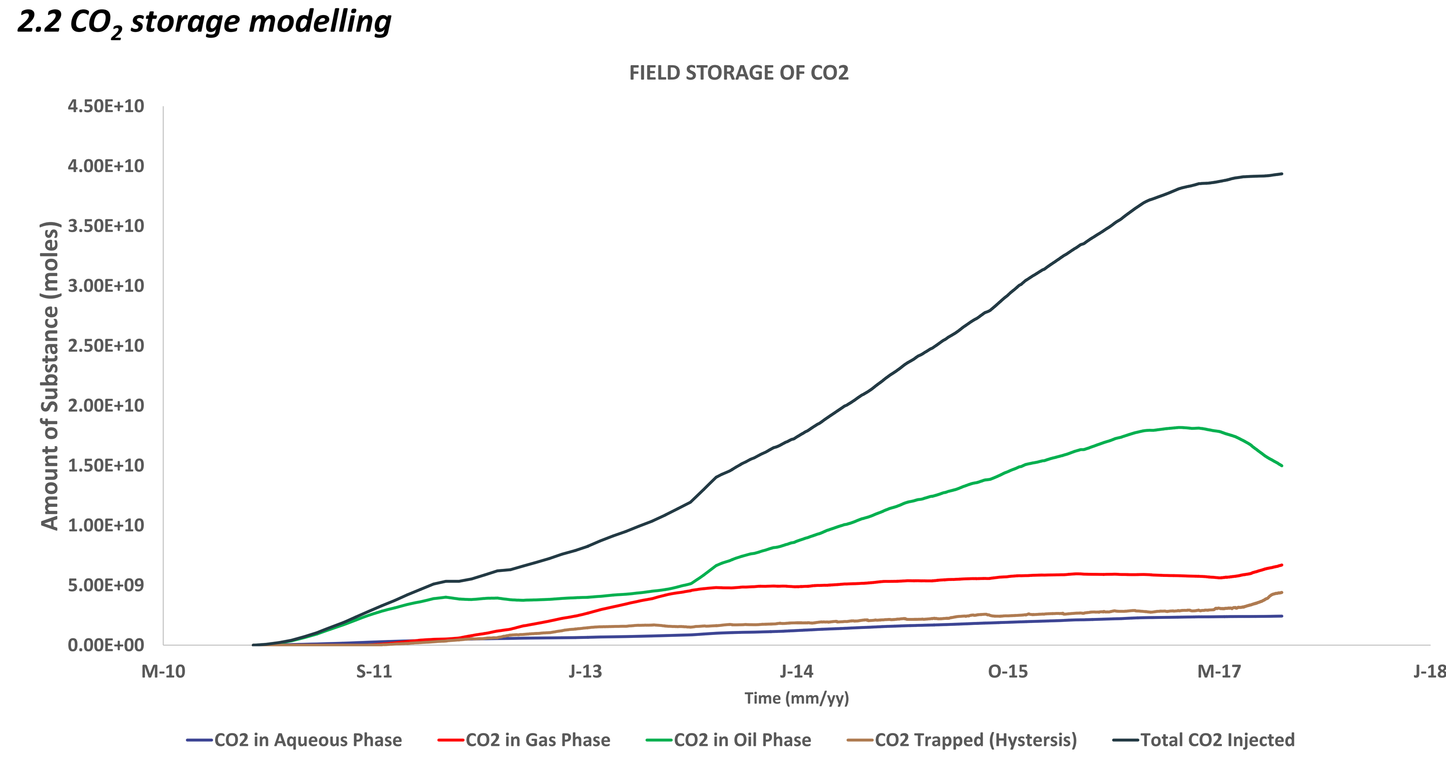

Figure 9. CO_2 storage profiles based on different trapping mechanisms within the Farnsworth Unit. It appears the amount of CO_2 stored is higher than the amount of CO_2 produced during EOR.

2.2.1 Phase distribution of Injected CO2

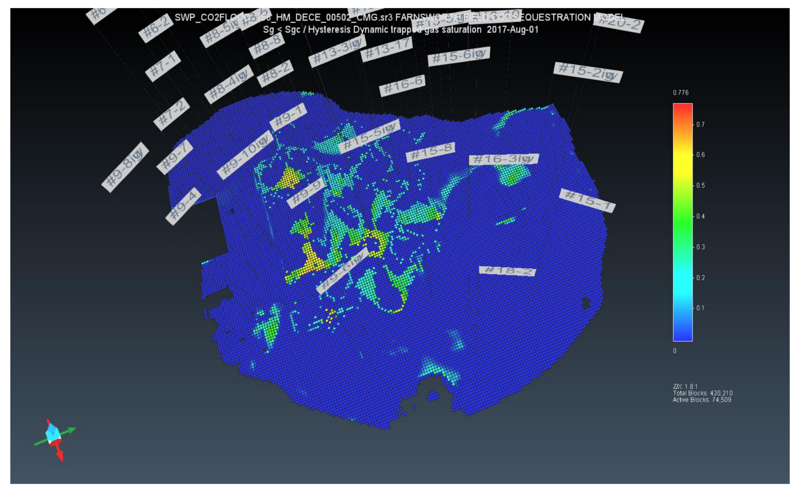
Figure 10. Hysteresis Gas Trapped Saturation

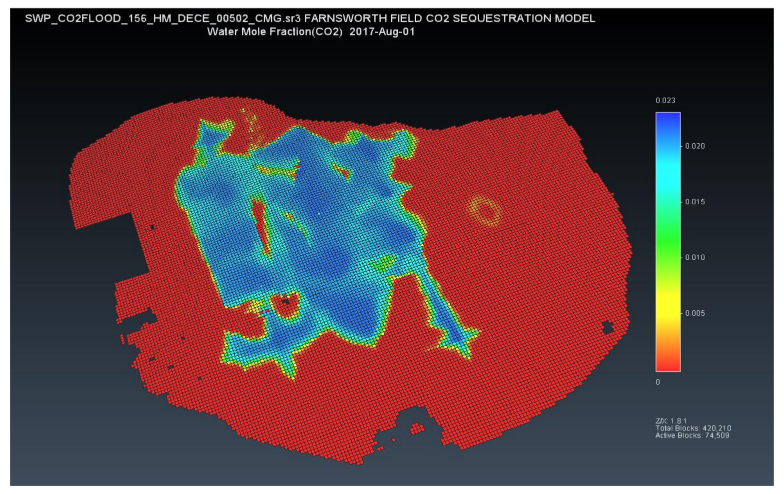
Figure 11. Water Mole Fraction (CO_2)

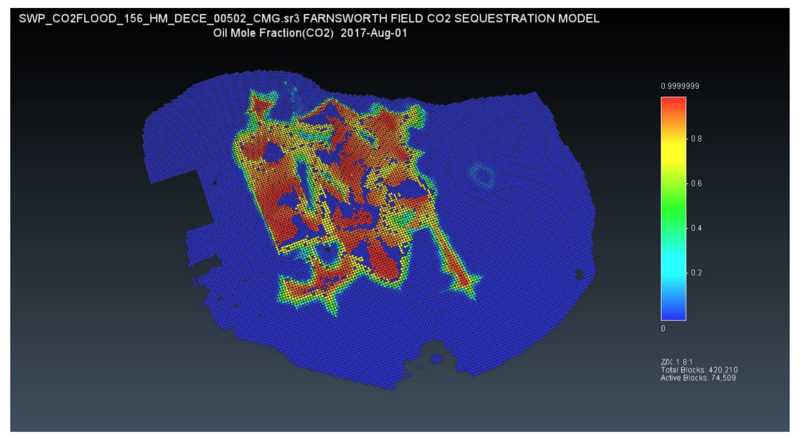
Figure 12. Oil Mole Fraction (CO_2)

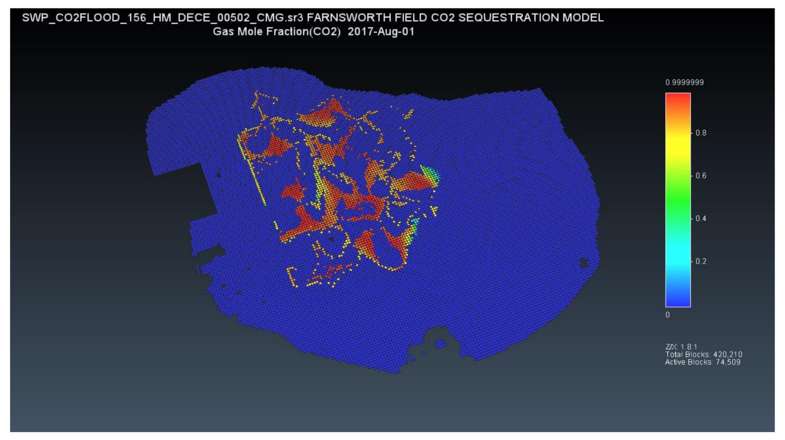
Figure 14. Gas Mole Fraction (CO_2)

2.3. GEOCHEMICAL SPECIATION MODELLING

Aqueous Species	Molality (mole/kg)
Al+++	1.96E-05
H3BO3(aq.)	3.99E-04
Ba++	7.14E-06
Br-	2.38E-04
Ca ++	8.91E-04
Cl-	4.67E-02
F-	4.12E-05
Fe++	6.53E-10
HCO3-	4.81E-01
K+	1.92E-04
Li+	5.36E-05
Mg++	3.82E-04
Na+	5.42E-02
So42-	1.79E-04
SeO32-	5.96E-07
SiO2 (aq.)	5.54E-04
Sr++	2.59E-05
Zn++	8.26E-07

Table 1. Pore water compositions OF FWU [5]

Principal FWU Mineral	Formula
Quartz	SiO_2
Albite	$NaAlSi_3O_8$
Calcite	$CaCO_3$
Dolomite	$Ca\,Mg(CO_3)_2$
Siderite	$FeCO_3$
Illite	$K_{0.6}\,Mg_{0.25}\,Al_{1.8}\,(\,Al_{0.5}\,Si_{3.5}\,O_{10}\,)(OH)_2$
Kaolinite	$Al_2\,Si_2\,O_5\,(OH)_4$
Smectite-clay	$Ca_{0.145}\,Mg_{0.26}\,Al_{1.77}\,Si_{3.97}\,O_{10}\,(OH)_2$
Chamosite	$Mg_{2.5}\,Fe_{2.5}\,Al_2Si_3O_{10}(OH)_8$

Table 2. Mineral Composition of the Morrow B Sandstone [4,5]

Table 1. List of all aqueous species from wells samples which are included as chemical equilibrium reactions in the intra-aqueous phase of the mineral trapping mechanism. Table 2 lists the principal minerals noted in the FWU Morrow B sandstone. These are minerals modelled as rate-dependent reactions, and it is expected to see evolution with dissolution/precipitation over a period of time.

CONCLUSION

The dissolution of CO_2 in the oil is found to be the predominant short-term CO_2 storage mechanism at FWU. As long as we keep injecting CO_2 above minimum miscibility pressure, a significant amount of the CO_2 will remain in the oil phase as compared to that as free gas and residual gas. However, over the course of years, the free gas will dissolve in the water phase thereby enhancing the amount stored in the aqueous phase. With the above trapping mechanisms modelled, a total of 39.4 BSCF was injected; 15.2 BSCF produced and 24.1 BSCF accumulated. Mineral trapping, a safe and permanent approach to storage, will be modelled in future work.

REFERENCES

1. Ampomah, W., Batch, R. S., Grigg, R. B., Dai, Z., & Pan, F. (2015). Compositional simulation of CO2 Storage Capacity in Depleted Oil Reservoirs. Carbon Management Technology Conference 2015: Sustainable and Economical CCUS Options, CMTC 2015, 1, 1–20.
2. Balch, R., McPherson, B., & Grigg, R. (2017). Overview of a Large Scale Carbon Capture, Utilization, and Storage Demonstration Project in an Active Oil Field in Texas, USA. Energy Procedia, 114(November 2016), 5874–5887. https://doi.org/10.1016/j.egypro.2017.03.1725
3. Munson, T. W. (1989). Depositional, Diagenetic, and Production History of the upper Morrowan Buckhaults Sandstone, Farnsworth Field Ochiltree County Texas. OCGS - The Shale Shaker Digest XIII, XXXX–XXXXI(1), 1–20.
4. Pan, F., McPherson, B. J., Esser, R., Xiao, T., Appold, M. S., Jia, W., & Moodie, N. (2016). Forecasting Evolution of Formation Water Chemistry and Long-term Mineral Alteration for GCS in a Typical Clastic Reservoir of the Southwestern United States. International Journal of Greenhouse Gas Control, 54, 524–537. https://doi.org/10.1016/j.ijggc.2016.07.035
5. Ahmmed, B., Appold, M. S., Fan, T., McPherson, B. J. O. L., Grigg, R. B., & White, M. D. (2016). Chemical Effects of Carbon Dioxide Sequestration in the Upper Morrow Sandstone in the Farnsworth, Texas, hydrocarbon unit. Environmental Geosciences, 23(2), 81–93. https://doi.org/10.1306/eg.09031515006
6. Larsen, J.A and Skauge A, "Methodology for Numerical Simulation with Cycle-Dependent Relative Permeabilities", SPE Journal, June 1998. SPE Paper # 38456.

ACKNOWLEDGEMENT

Funding for this project is provided by the U.S. Department of Energy's (DOE) National Energy Technology Laboratory (NETL) through the Southwest Regional Partnership on Carbon Sequestration (SWP) under Award No. DE-FC26-05NT42591.

Eusebius Jr. Kutsienyo (eusebiusjunior.kutsienyo@student.nmt.edu)
William Ampomah (William.ampomah@nmt.edu)